Compact Capacitively-Loaded Transmission Line with Enhanced Phase Shift Range

Zulfi[1,2]
[1]*Radio Telecomm. and Microwave Lab.*
School of Electrical Eng. & Informatics, ITB
[2]*School of Electrical Eng., Telkom University*
Bandung, Indonesia
zulfi@students.stei.itb.ac.id

Joko Suryana
Radio Telecomm. and Microwave Lab.
School of Electrical Eng. & Informatics
Institut Teknologi Bandung
Bandung, Indonesia
joko.suryana@itb.ac.id

Achmad Munir
Radio Telecomm. and Microwave Lab.
School of Electrical Eng. & Informatics
Institut Teknologi Bandung
Bandung, Indonesia
munir@ieee.org

***Abstract*—Capacitively-loaded transmission line realized using a common configuration has typically a narrow phase shift range, so it is unusable as a phase shifter for beamforming applications. Increasing the number of capacitors to enhance the phase shift range is usually accompanied by an increase in the transmission line section, resulting in a large circuit size. This paper presents an implementation of a mirror configuration on a capacitor-loaded microstrip line to enhance the phase shift range. The loading capacitors are located on both sides of the transmission line section, instead of being located on one side. The experimental results show that when capacitances are varied from 0.2 pF to 0.8 pF, the proposed configuration could produce a wide phase shift range of 139.48^{o} and a compact circuit size of 46.4 mm $\times$ 22.5 mm. The capacitively-loaded transmission line implemented using a mirror configuration increases the phase shift range by 55% and reduces the circuit size by 22% compared to the common configuration.**

***Index Terms*—loaded-line; phase shifter; beamforming; mirror configuration; capacitor.**

I. Introduction

The tremendous growth of mobile phone gadgets and their applications has resulted in a significant increase in wireless data traffic. In order to satisfy the demand, the capacity of wireless communication network must be further expanded. However, active subscriber movement and interference issues arise, especially in femtocell-based networks [1], yielding in degraded signal quality and reduced system throughput. To overcome this challenge, beamforming phased-array antennas [2] emerge as a potential candidate for emerging wireless communication networks as they have the ability to generate a large number of directional beams and point them in the direction of the macrocell and femtocell users, leading to an enhanced signal to interference plus noise ratio (SINR). Phase shifters are essential for multibeam antennas to provide phase differences among adjacent array elements. However, they must satisfy the stringent requirements, i.e., continuously tunable phase, simple control circuit, negligible direct current (DC) energy consumption, and low-cost.

During the last decade, passive phase shifters have been designed using different configurations such as switched line, reflection type, and loaded line. Switched-based phase shifters provide non-continuous phase shifts. Whilst reflection-based phase shifters enable continuous phase shifts, however their circuit dimensions are typically large due to the use of couplers, especially at low frequencies. The loaded-line configurations are commonly comprised of high-impedance line sections and capacitors with variable capacitance. Different phase shifts can be obtained by varying the capacitances, which can be realized by complementary-metal-oxide-semiconductor (CMOS), micro-electro-mechanical-system (MEMS), and ferroelectric technologies. Varactors are frequently used as capacitive elements since they feature fast-switching times, light weight, and low cost [3]. The varactor-loaded line configuration has several desirable features satisfying the requirements for passive beamforming antenna applications. It provides continuous phase shift with only requiring a single control/biased line, and the circuit consumes insignificant DC power.

Loaded-line configurations could be implemented by many types of lines, such as coplanar waveguides (CPW) [4], [5], lumped elements [6], metamaterials [7], [8], and half-mode substrate integrated waveguide (HMSIW) [9]. Among the aforementioned lines, CPW is typically applied for loaded-line structures as both signal and ground lines are on the same plane, which makes easier in the implementation. However, loaded-CPW phase shifters occupy significant resources leading to high-cost implementation. Several loaded-microstrip line phase shifters have been realized using common configuration [10]–[12], unfortunately their phase shifting ranges were limited. In the current work, a mirror configuration is adopted to broaden the phase shifting range of a capacitively-loaded transmission line. Loading capacitors are located on both sides of the transmission line section, instead of only being located on one side. It will be demonstrated that capacitively-loaded transmission line using a mirror configuration can generate a broader phase shift range compared to the common configuration while preserving a good match over the entire bandwidth coverage. In addition, a compact circuit size is also presented. Section II discusses capacitively-loaded transmission line theory and configuration. Section III describes fabrication and measurement. Section IV provides concluding remarks.

II. Capacitively-Loaded Transmission Line

A. Theoretical Analysis

Fig. 1(a) depicts a schematic of capacitively-loaded transmission line which consists of a number of transmission line sections with the line length of θ, line impedance of Z, and loaded by capacitors with capacitance of C. The structure can be considered as a cascaded arrangement of capacitors and transmission line sections. The transmission matrix of such arrangement can be determined by multiplying transmission matrices of the capacitor and the line section. For the case of three cascaded arrangements, i.e., four capacitors and three line sections, the transmission matrix of capacitively-loaded transmission line can be written as (1).

$$\begin{aligned}\begin{bmatrix} A & B \\ C & D \end{bmatrix} = &\begin{bmatrix} 1 & 0 \\ j\omega C & 1 \end{bmatrix} \begin{bmatrix} \cos\theta & jZ\sin\theta \\ \dfrac{j\sin\theta}{Z} & \cos\theta \end{bmatrix} \\ &\begin{bmatrix} 1 & 0 \\ j\omega C & 1 \end{bmatrix} \begin{bmatrix} \cos\theta & jZ\sin\theta \\ \dfrac{j\sin\theta}{Z} & \cos\theta \end{bmatrix} \\ &\begin{bmatrix} 1 & 0 \\ j\omega C & 1 \end{bmatrix} \begin{bmatrix} \cos\theta & jZ\sin\theta \\ \dfrac{j\sin\theta}{Z} & \cos\theta \end{bmatrix} \begin{bmatrix} 1 & 0 \\ j\omega C & 1 \end{bmatrix} \end{aligned} \quad (1)$$

As is already known that the configuration of loaded transmission line is basically a periodic structure that has a cut-off frequency [13]. For working frequencies much lower than the cut-off frequency, the matrix in (1) equals to a transmission matrix of unloaded transmission line depicted in Fig. 1(b) which is given by (2) [14].

$$\begin{bmatrix} A_0 & B_0 \\ C_0 & D_0 \end{bmatrix} = \begin{bmatrix} \cos\theta_0 & jZ_0\sin\theta_0 \\ \dfrac{j\sin\theta_0}{Z_0} & \cos\theta_0 \end{bmatrix} \quad (2)$$

where Z_0 is line impedance and θ_0 is electrical length of unloaded transmission line. By equating (1) and (2), the relationship between loaded line parameters can be obtained. For the case of three cascaded arrangements, the relationship of θ_0 can be expressed in (3).

$$\theta_0 = arcsin\left[\frac{Z\sin\theta}{Z_0}(CZ\omega\sin\theta - 2\cos\theta)^2 - 1\right] \quad (3)$$

From (3), it is obviously seen that the controllable θ_0 with constant Z_0 can be achieved by varying the capacitance. Based on this property, the capacitively-loaded transmission line can be used to construct a tunable phase shifter.

Fig. 2(a) illustrates a schematic of capacitively-loaded transmission line with three cascaded arrangements. The schematic is symmetric with respect to *PP'* plane, and hence the even-odd mode method can be applied to determine the s-cattering parameters. The corresponding even- and odd-mode networks are depicted in Figs. 2(b) and 2(c), respectively. For both modes, the even input impedance (Z_{even}) and the odd input impedance (Z_{odd}) can be written as (4) and (5), respectively.

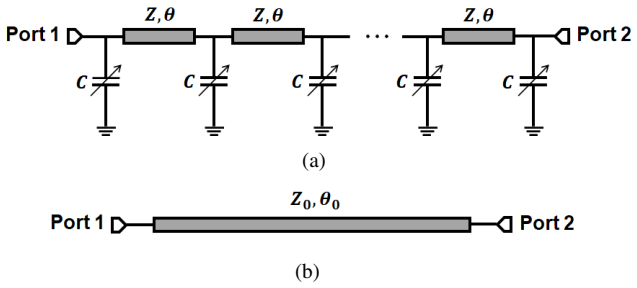

Fig. 1. Schematic of (a) capacitively-loaded transmission line, (b) unloaded transmission line.

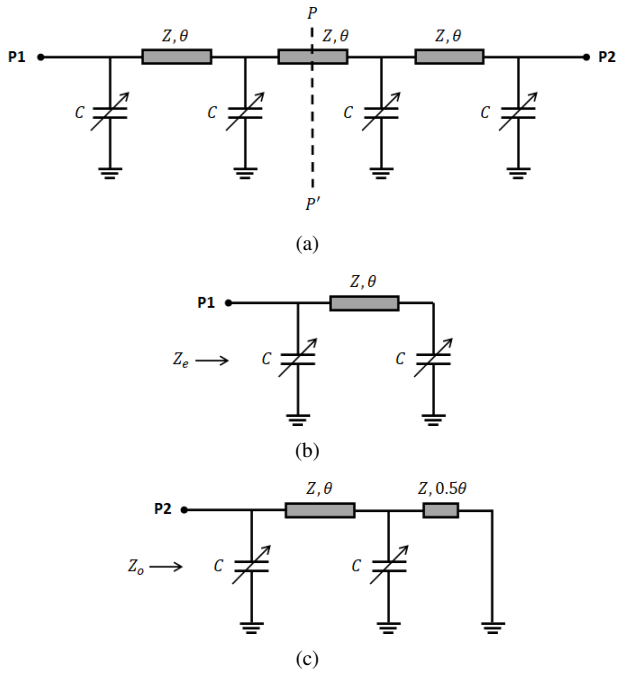

Fig. 2. Schematic of (a) Capacitively-loaded transmission line with three line section and four capacitor, (b) even-mode of (a), (b) odd-mode of (a).

$$Z_{even} = (1/j\omega C)||Z\frac{(1/j\omega C) + jZ\tan(\theta)}{Z + j(1/\omega C)\tan(\theta)} \quad (4)$$

$$Z_{odd} = \left(\frac{1}{j\omega C}\right)||Z\frac{[(1/j\omega C)||jZ\tan(0.5\theta)] + jZ\tan(\theta)}{Z + j[(1/j\omega C)||jZ\tan(0.5\theta)]\tan(\theta)} \quad (5)$$

Based on the even- and odd- impedances in (4) and (5), the reflection coefficients of even- and odd-mode can be calculated as given by (6) and (7), respectively.

$$\Gamma_{even} = \frac{Z_{even} - Z_{port}}{Z_{even} + Z_{port}} \quad (6)$$

$$\Gamma_{odd} = \frac{Z_{odd} - Z_{port}}{Z_{odd} + Z_{port}} \quad (7)$$

where Z_{port} is a port impedance of 50 Ω. Furthermore, the scattering parameters of capacitively-loaded transmission line in Fig. 2(a) can be calculated using (8) and (9).

$$S_{11} = S_{22} = 0.5(\Gamma_{even} + \Gamma_{odd}) \quad (8)$$

$$S_{21} = S_{12} = 0.5(\Gamma_{even} - \Gamma_{odd}) \quad (9)$$

B. Common Configuration

Fig. 3 depicts the layout of capacitively-loaded microstrip line designed using a common configuration which consists of four loading capacitors and three high-impedance line sections. In this configuration, loading capacitors are located on one side of microstrip line sections. Here, a via hole is utilized to connect each capacitor to the groundplane. The configuration is deployed on a 1.6 mm thick FR4 epoxy dielectric substrate with the relative permittivity of 4.3 and the loss tangent of 0.02. The characteristic impedance and the electrical length of microstrip line section are set to be 75 Ω and 60°, respectively. Meanwhile the capacitance of loading capacitors is varied in the range of 0.2 pF–0.8 pF. The optimized layout dimensions of common configuration are tabulated in Table I.

The simulation results of scattering parameters, including phase shift, insertion loss, and return loss of the common configuration are plotted in Figs. 4–6. As shown in Fig. 4, the phase shift range is 86° at the frequency of 2.4 GHz. Meanwhile, the minimum insertion loss and the variation of insertion loss as depicted in Fig. 5 are 1.2 dB and 0.7 dB, respectively. It is seen that the return losses are better than 10 dB in a frequency range from 1.9 GHz to 2.9 GHz, as indicated in Fig. 6. Although the common configuration achieved a good insertion loss and return loss, however the phase shift range is narrow for the desired application.

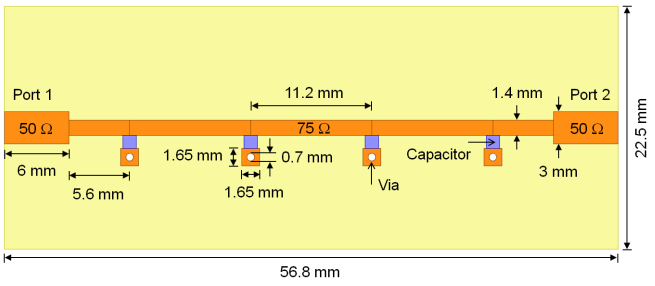

Fig. 3. Layout of capacitively-loaded microstrip line designed using common configuration.

TABLE I
OPTIMIZED LAYOUT DIMENSIONS OF COMMON CONFIGURATION.

Parameter	Dimension (mm)
Length of microstrip line section	11.2
Width of microstrip line section	1.4
Length of capacitor pad	1.2
Width of capacitor pad	1.25
Length of via	1.65
Width of via	1.65
Diameter of hole	0.7

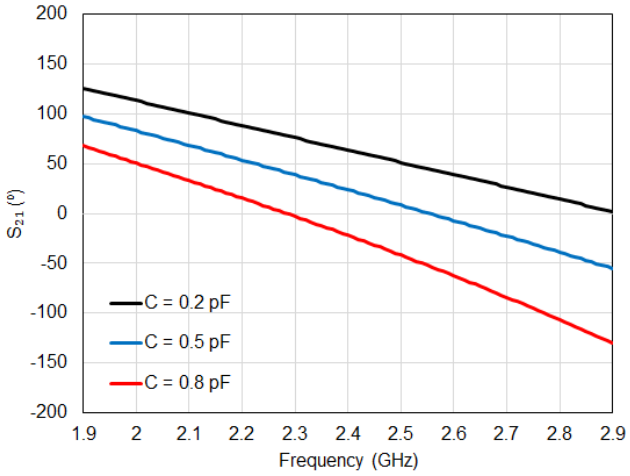

Fig. 4. Simulated phase response of common configuration.

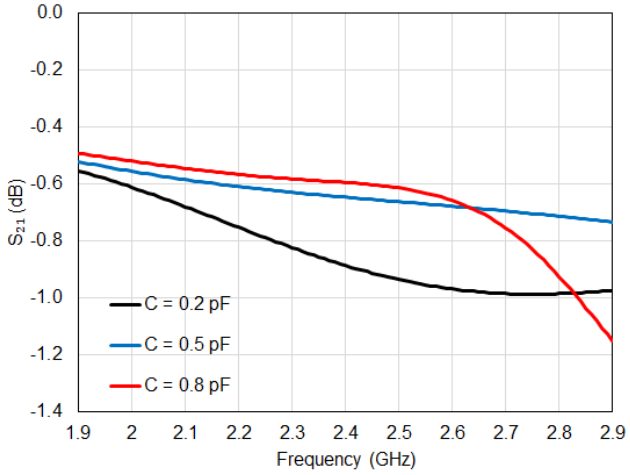

Fig. 5. Simulated insertion losses of common configuration.

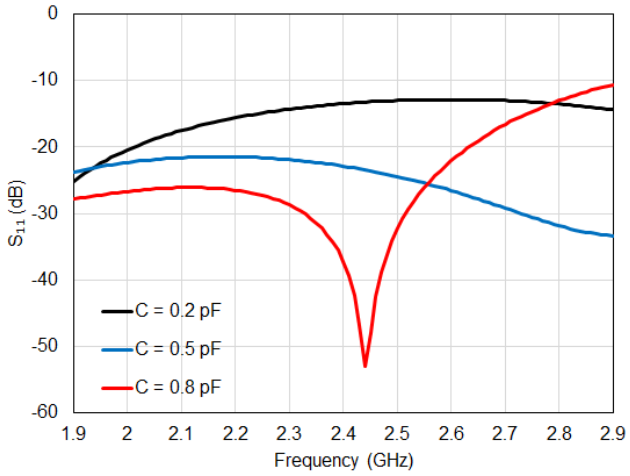

Fig. 6. Simulated return losses of common configuration.

C. Proposed Configuration

The schematic of proposed capacitor-based transmission line is shown in Fig. 7. The mirror configuration in [15], [16] is applied to increase the phase shifting range in the frequency band of operation. In contrast to the common configuration, loading capacitors are located on both sides of the transmission line section. The design procedure in [3] is adopted to achieve low insertion loss and less variation of insertion loss at the desired operation frequency.

Fig. 8 shows the layout of proposed phase shifter designed using mirror configuration. Similar to the common configuration, the proposed transmission line structure was designed on an FR4 epoxy dielectric substrate with the thickness of 1.6 mm. The width and length of microstrip line section are 1.4 mm and 8.6 mm, respectively, which correspond to the characteristic impedance (Z) of 75 Ω and the electrical length (θ) of 45.6°, respectively. The diameter of each via hole is set to be 0.7 mm, and a square patch on the top of via has the size of 1.65 mm.

The proposed configuration has been simulated in the frequency range from 1.9 GHz to 2.9 GHz. The capacitor pad is represented as a rectangular patch with the length of 1.2 mm and the width of 1.25 mm, which corresponds to the footprint of 0805 surface-mount device (SMD) component. The simulations were performed for a range of capacitance from 0.2 pF–0.8 pF, which correlates to a capacitance range of MA46H120 type varactor diode [17]. The dimensions of microstrip line section are optimized for gaining the maximum phase shift range and the minimum insertion loss when the capacitance is varied. The optimum dimensions of proposed layout configuration are listed in Table II.

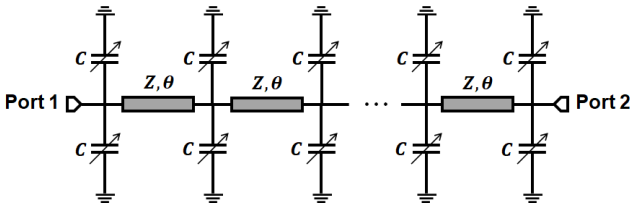

Fig. 7. Schematic of capacitor-based transmission line using mirror configuration.

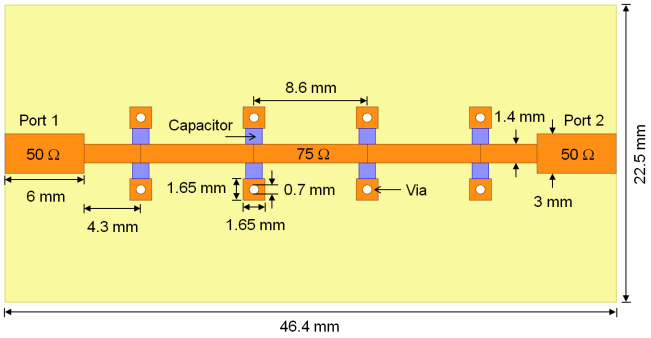

Fig. 8. Layout of proposed phase shifter designed based on capacitively-loaded transmission line using mirror configuration.

TABLE II
OPTIMUM DIMENSIONS OF PROPOSED CONFIGURATION.

Parameter	Dimension (mm)
Length of microstrip line section	8.6
Width of microstrip line section	1.4
Length of patch	1.65
Width of patch	1.65
Length of capacitor pad	1.2
Width of capacitor pad	1.25
Length of via	1.65
Width of via	1.65
Diameter of via hole	0.7

III. Circuit Fabrication and Measurement

Fig. 9 depicts the fabricated phase shifter realized based on capacitively-loaded transmission line using the proposed configuration. It was implemented on an FR4 epoxy dielectric substrate with the thickness of 1.6 mm. High-frequency multilayer ceramic capacitors (MLCC) from Murata Electronics are used as variable capacitors. A 50 Ω connector is attached and soldered at each port of the realized phase shifter for characteristics measurement. A Cobalt C1220 vector network analyzer (VNA) from Copper Mountain Technologies is utilized for measuring its characteristics. Some key parameters, including transmission phase, insertion loss, and return loss, are measured for a 0.2 pF–0.8 pF capacitance range over a 1.9 GHz–2.9 GHz frequency range. The results of measurement and simulation are plotted in Figs. 10–12.

As shown in Fig. 10, the measured and simulated phase responses are consistent each other across the frequency range of observations. At the frequency of 2.4 GHz, when the capacitance is varied from 0.2 pF to 0.8 pF, the measured phase changes from 91.14° to –48.34°, which corresponds to a 139.48° phase shift range, while the simulated phase changes from 95.34° to –37.75°, resulting in a 133.10° phase shift range. There is a slight discrepancy between the measured and simulated results which are mainly due to the capacitance offset. The greater the capacitance, the greater the phase difference. For the same capacitance tolerance, the greater the capacitance, the greater the capacitance offset. Moreover, the connectors attached at the input and output ports for the measurement could also lead to a phase leg.

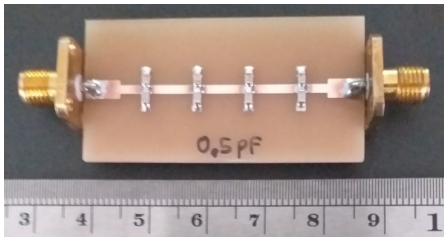

Fig. 9. Fabricated phase shifter realized based on capacitively-loaded transmission line using mirror configuration.

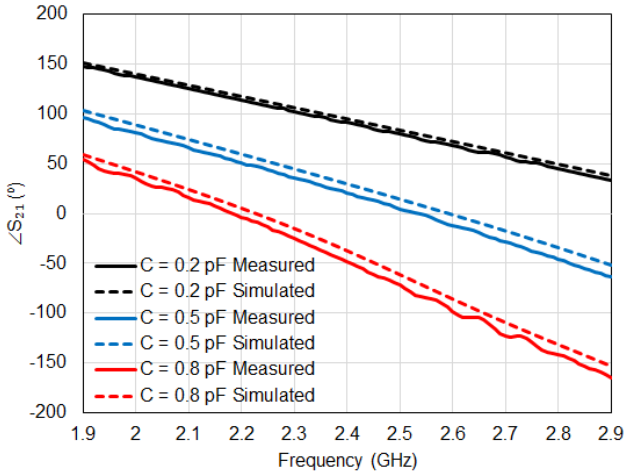

Fig. 10. Comparison of measured and simulated phase responses.

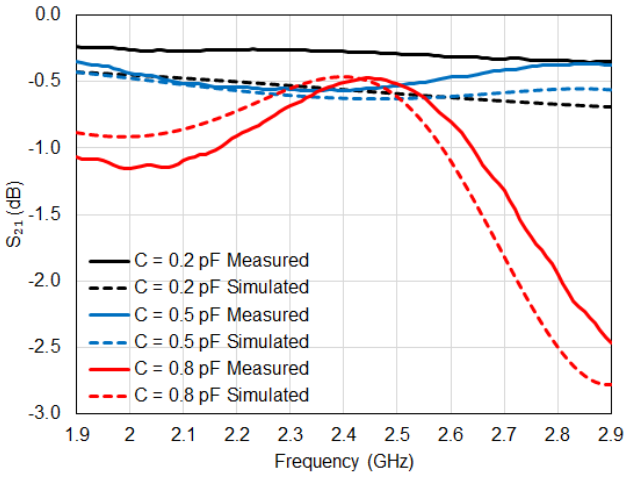

Fig. 11. Comparison of measured and simulated insertion losses.

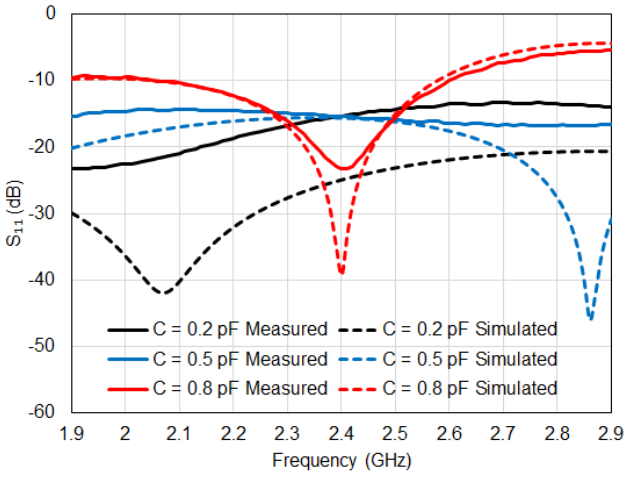

Fig. 12. Comparison of measured and simulated return losses.

TABLE III
PERFORMANCES OF PHASE SHIFTER AT 2.4 GHZ USING PROPOSED CONFIGURATION.

Parameter	Measurement	Simulation
Phase shift range (°)	139.48	133.10
Maximum insertion loss (dB)	0.52	0.62
Insertion loss variation (dB)	0.2	0.3
Return loss (dB)	15.33	15.53
Fractional bandwidth (%)	22.08	21.05

Fig. 11 depicts the comparison of measured and simulated insertion losses across the frequency observations. There is good agreement between measurement and simulation results. The maximum insertion loss is about 3 dB in the frequency range from 1.9 GHz to 2.9 GHz. As expected, the variation of minimum insertion losses occurred around the center frequency of 2.4 GHz. It shows that the measured results at the frequency of 2.4 GHz indicate minimum and maximum insertion losses of 0.32 dB and 0.52 dB, respectively, which corresponds to a 0.2 dB insertion loss variation. Whilst the simulated results have a 0.3 dB insertion loss variation from a minimum of 0.32 dB to a maximum of 0.62 dB. A slight difference between measurement and simulation results is possibly attributed to connector losses and fabrication tolerance.

Furthermore, the comparison of measured and simulated return losses across the frequency observation is plotted in Fig. 12. The measured return losses are less than –10 dB over a 530 MHz bandwidth ranging from 2.06 GHz to 2.59 GHz, which correlates to a 22.08% fractional bandwidth. Whereas the simulated return losses are less than –10 dB over a 510 MHz bandwidth ranging from 2.06 GHz to 2.57 GHz, which corresponds to a 21.25% fractional bandwidth. At the frequency of 2.4 GHz, the measured and simulated return losses are 15.33 dB and 15.53 dB, respectively. Table III compares the results of measurement and simulation for several key performance metrics of phase shifter. It is clear that a capacitively-loaded transmission line implemented with a mirror configuration could achieve a wide phase shift range, low insertion loss, low variation of insertion loss, and good match over a wide bandwidth response.

IV. CONCLUSION

A compact phase shifter developed based on capacitively-loaded transmission line using a mirror configuration has been presented. To enhance the phase shift range while preserving the circuit size, loading capacitors are located on both sides of the transmission line sections. A prototype of phase shifter operating at the frequency of 2.4 GHz has been realized and characterized for experimental verification. The measurements have indicated that the proposed configuration yielded a 55% greater phase shift range and a 22% smaller circuit size compared to the common configuration. The insertion loss, the variation of insertion loss, and the bandwidth response were comparable for both configurations.

REFERENCES

[1] A. A. Bathich, S. I. Suliman, H. M. A. Hj. Mansor, S. G. A. Ali, and R. Abdulla, "Cell selection mechanism based on Q-learning environment in femtocell LTE-A networks," *J. ICT Res. Appl.*, vol. 15, no. 1, pp. 56–70, Jul. 2021. DOI: 10.5614/itbj.ict.res.appl.2021.15.1.4

[2] È. Amyotte, Y. Demers, L. Hildebrand, S. Richard, and S. Mousseau, "A review of multibeam antenna solutions and their applications," in *Proc. 8th European Conference on Antennas and Propagation (EuCAP 2014)*, The Hague, Netherlands, Apr. 2014, pp. 191–195, DOI: 10.1109/EuCAP.2014.6901724.

[3] A. S. Nagra, Jian Xu, E. Erker, and R. A. York, "Monolithic GaAs phase shifter circuit with low insertion loss and continuous 0-360/spl deg/ phase shift at 20 GHz," *Microw. Guided Wave Lett.*, vol. 9, no. 1, pp. 31–33, Jan. 1999, DOI: 10.1109/75.752115.

[4] R. Bourtoutian and P. Ferrari, "Tapered distributed analogue tunable phase shifter with low insertion and return loss," *Electron. Lett.*, vol. 41, no. 15, pp. 852–854, Jul. 2005, DOI: 10.1049/el:20051810.

[5] M. Ould-Elhassen, M. Mabrouk, A. Ghazel, and P. Benech, "Comparative measurements of tapering input effects on tunable distributed phase shifter performances," in *Proc. 11th Mediterranean Microwave Symposium (MMS)*, Yasmine Hammamet, Tunisia, Sep. 2011, pp. 314–318, DOI: 10.1109/MMS.2011.6068588.

[6] F. Ellinger, H. Jackel, and W. Bachtold, "Varactor-loaded transmission-line phase shifter at C-band using lumped elements," *IEEE Trans. Microw. Theory Tech.*, vol. 51, no. 4, pp. 1135–1140, Apr. 2003, DOI: 10.1109/TMTT.2003.809670.

[7] L.-Q. Ma, F.-Y. Meng, X.-X. Liu, and P.-Y. Wang, "An S-band left-handed tunable phase shifter based on BST thin film," in *3rd Asia-Pacific Conference on Antennas and Propagation (APCAP)*, Harbin, China, Jul. 2014, pp. 1389–1391, DOI: 10.1109/APCAP.2014.6992784.

[8] P. Li et al., "A novel 360º continuously tunable phase shifter based on varactor-loaded CRLH transmission line at exact 2.4 GHz," in *Proc. IEEE International Conference on Electronic Information and Communication Technology (ICEICT)*, Harbin, China, Aug. 2016, pp. 583–585, DOI: 10.1109/ICEICT.2016.7879773.

[9] Z. Taha, H. Jassim, A. Ahmed, and I. Farhan, "Design and implementation of triple band half mode substrate integrated waveguide (HMSIW) antenna with compact size," *J. ICT Res. Appl.*, vol. 15, no. 2, pp. 120–138, Oct. 2021, DOI: 10.5614/itbj.ict.res.appl.2021.15.2.2.

[10] H. Ren, M. Zhou, Y. Gu, and B. Arigong, "A tunable transmission line with controllable phase shifting and characteristic impedance," *IEEE Trans. Circuits Syst. II, Exp. Briefs*, vol. 67, no. 10, pp. 1720–1724, Oct. 2020, DOI: 10.1109/TCSII.2019.2946307.

[11] G. Yang, C. S. Lee, M. Ezzat, and L. Zhang, "A novel tunable phase shifter with distributed capacitive loading," in *Proc. IEEE Texas Symposium on Wireless and Microwave Circuits and Systems (WMCS)*, Waco, USA, May 2021, pp. 1–4, DOI: 10.1109/WMCS52222.2021.9493281.

[12] Zulfi, J. Suryana, and A. Munir, "Characterization of capacitor-loaded transmission line for phase shifter application," in *Proc. International Workshop on Antenna Technology (iWAT)*, Dublin, Ireland, May 2022, pp. 17–20, DOI: 10.1109/iWAT54881.2022.9810901.

[13] D. Salameh and D. Linton, "Microstrip GaAs nonlinear transmission-line (NLTL) harmonic and pulse generators," *IEEE Trans. Microw. Theory Tech.*, vol. 47, no. 7, pp. 1118–1122, Jul. 1999, DOI: 10.1109/22.775445.

[14] D. K. Misra, *Radio-Frequency and Microwave Communication Circuits: Analysis and Design*, New Jersey, USA: Wiley, 2004, pp. 298–304, DOI: 10.1002/0471653764.

[15] L. Pierantoni et al., "Broadband microwave attenuator based on few layer graphene flakes," *IEEE Trans. Microw. Theory Tech.*, vol. 63, no. 8, pp. 2491–2497, Aug. 2015, DOI: 10.1109/TMTT.2015.2441062.

[16] M. Yasir, S. Bistarelli, A. Cataldo, M. Bozzi, L. Perregrini, and S. Bellucci, "Voltage-controlled and input-matched tunable microstrip attenuators based on few-layer graphene," *IEEE Trans. Microw. Theory Tech.*, vol. 68, no. 2, pp. 701–710, Feb. 2020, DOI: 10.1109/TMTT.2019.2953611.

[17] MACOM Technology Solutions, MA46H120 Varactor Datasheet [Online]. Available: https://cdn.macom.com/datasheets/MA46H120 Series.pdf, accessed on: Jun. 19, 2022.